Title

Epigenetic Regulation of NGF-Mediated Osteogenic Differentiation in Human Dental Mesenchymal Stem Cells

Journal

Stem Cells, 40(9)

ISSN

1066-5099

Authors

Liu, Zhenqing
Suh, Jin Sook
Deng, Peng
et al.

Publication Date

2022-09-26

DOI

10.1093/stmcls/sxac042

Peer reviewed

Stem Cells, 2022, **40**, 818–830
https://doi.org/10.1093/stmcls/sxac042
Advance access publication 21 June 2022
Original Research

Epigenetic Regulation of NGF-Mediated Osteogenic Differentiation in Human Dental Mesenchymal Stem Cells

Zhenqing Liu[1], Jin Sook Suh[2], Peng Deng[1], Olga Bezouglaia[3], Megan Do[4], Mojan Mirnia[5], Zhong-Kai Cui[6], Min Lee[6,7], Tara Aghaloo[3], Cun-Yu Wang[1,7,8], Christine Hong[2,8]

[1]Division of Oral Biology and Medicine, School of Dentistry, University of California, Los Angeles (UCLA), Los Angeles, CA, USA
[2]Department of Orofacial Sciences, School of Dentistry, University of California, San Francisco (UCSF), San Francisco, CA, USA
[3]Division of Diagnostic and Surgical Sciences, School of Dentistry, University of California, Los Angeles (UCLA), Los Angeles, CA, USA
[4]School of Dentistry, University of California, San Francisco (UCSF), San Francisco, CA, USA
[5]School of Dentistry, University of California, Los Angeles (UCLA), Los Angeles, CA, USA
[6]Division of Advanced Prosthodontics, School of Dentistry, University of California, Los Angeles (UCLA), Los Angeles, CA, USA
[7]Department of Bioengineering, University of California, Los Angeles (UCLA), Los Angeles, CA, USA

[8]Corresponding author: Cun-Yu Wang, DMD, PhD, UCLA School of Dentistry, CHS 33-030, 10833 Le Conte Ave, Los Angeles, CA 90095, USA. Tel: +1 310 825 4415; Email: cwang@dentistry.ucla.edu; or, Christine Hong, DMD, MS, UCSF School of Dentistry, D1013, 707 Parnassus Ave, San Francisco, CA 94143, USA. Tel: +1 415 514 7413; Email: yeumin.hong@ucsf.edu

Abstract

Nerve growth factor (NGF) is the best-characterized neurotrophin and is primarily recognized for its key role in the embryonic development of the nervous system and neuronal cell survival/differentiation. Recently, unexpected actions of NGF in bone regeneration have emerged as NGF is able to enhance the osteogenic differentiation of mesenchymal stem cells. However, little is known regarding how NGF signaling regulates osteogenic differentiation through epigenetic mechanisms. In this study, using human dental mesenchymal stem cells (DMSCs), we demonstrated that NGF mediates osteogenic differentiation through $p75^{NTR}$, a low-affinity NGF receptor. $P75^{NTR}$-mediated NGF signaling activates the JNK cascade and the expression of KDM4B, an activating histone demethylase, by removing repressive H3K9me3 epigenetic marks. Mechanistically, NGF-activated c-Jun binds to the KDM4B promoter region and directly upregulates KDM4B expression. Subsequently, KDM4B directly and epigenetically activates DLX5, a master osteogenic gene, by demethylating H3K9me3 marks. Furthermore, we revealed that KDM4B and c-Jun from the JNK signaling pathway work in concert to regulate NGF-mediated osteogenic differentiation through simultaneous recruitment to the promoter region of DLX5. We identified KDM4B as a key epigenetic regulator during the NGF-mediated osteogenesis both in vitro and in vivo using the calvarial defect regeneration mouse model. In conclusion, our study thoroughly elucidated the molecular and epigenetic mechanisms during NGF-mediated osteogenesis.

Key words: NGF; KDM4B; osteogenesis; human dental mesenchymal stem cells; bone regeneration; epigenetics.

Graphical Abstract

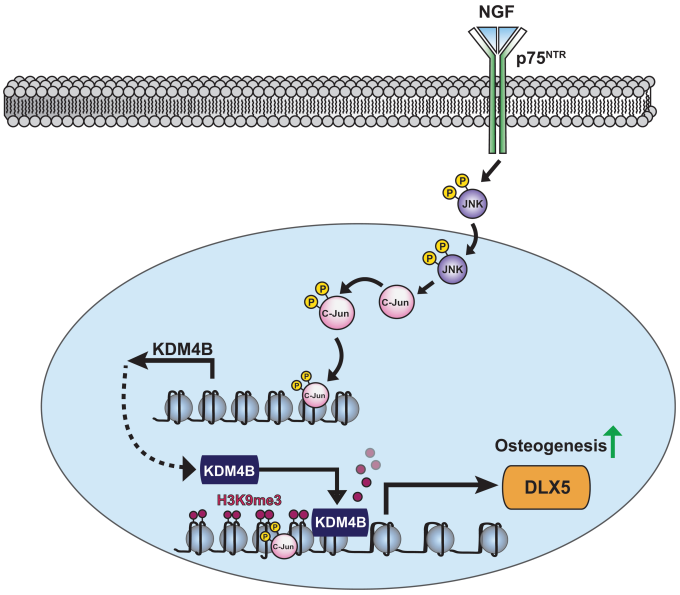

Received: 20 January 2022; Accepted: 2 June 2022.

Significance Statement

Recently, nerve growth factor (NGF) has become recognized as a potential player in inducing osteogenesis. However, the molecular mechanism of NGF signaling in bone has been largely unknown. In this current study, we examined the role of molecular and epigenetic regulation in NGF-mediated osteogenic differentiation of human dental mesenchymal stem cells (DMSCs) and bone regeneration in calvarial defects. $p75^{NTR}$-mediated NGF signaling activates the JNK cascade and the expression of KDM4B, an activating histone demethylase, by removing repressive H3K9me3 epigenetic marks. Our findings are significant in stem cell biology as KDM4B may serve as a novel therapeutic target in bone regeneration.

Introduction

Craniofacial defects encompass a wide range of conditions from congenital anomalies to diseases such as cancer and mechanical trauma to the head and neck region. Such defects affect the daily functioning and psychosocial well-being of individuals affected due to the facial region's vital functions in appearance, communication, and eating. Stem cell-based tissue engineering has emerged as one of the most promising approaches to restoring intact craniofacial bone tissues.[1] Current studies using various types of mesenchymal stem cells (MSCs) have demonstrated great promise for use in cell-mediated therapy for craniofacial regeneration.[2-4]

MSCs derived from dental tissues (DMSCs) are particularly suited for craniofacial regeneration due to their identical embryonic origins to the injured site. DMSCs have additional advantages over the most widely utilized MSCs isolated from adult bone marrow (BMSCs), as they are more readily available from discarded dental tissues and exhibit higher clonogenic and proliferative potential than BMSCs.[5] Research indicates that DMSCs can differentiate into osteoblasts under osteogenic conditions[6] and regenerate bone tissues in vivo.[7,8] However, the selective isolation of highly regenerative MSCs from dental tissues is critical for their successful use in clinical settings. Our recent work in isolating homogenous populations of DMSCs using cell surface marker expression revealed that CD271 was the most effective marker for isolating DMSCs with high osteogenic potential. CD271, also known as $p75^{NTR}$, is a nerve growth factor (NGF) receptor that has been described as a bona fide neural crest stem cell marker and one of the most reliable surface markers for isolation of putative BMSCs.[5]

Nerve growth factor is the best-characterized neurotrophin and is primarily recognized for its key role in the embryonic development of the nervous system and neuronal cell survival/differentiation.[9,10] However, the unanticipated plurality of NGF actions in cells other than nerve cells has been increasingly elucidated, expanding the biology of NGF. Studies have reported that NGF and its receptors are implicated in inflammation, bone resorption, and the acceleration of wound healing in the skin of mice.[11-13] It has been shown that NGF treatment could promote MSC fate toward neural lineages in an induced medium while NGF secreted from MSCs enhances neural stem cell differentiation.[14,15] Interestingly, emerging evidence suggests that NGF induces osteogenic differentiation and bone formation.[16,17]

The physiological effects of NGF are mediated by one of two membrane receptors, TrkA and $p75^{NTR}$, or both concurrently.[18] Nerve growth factor is able to activate multiple signaling pathways including AKT,[19] Ras-mediated mitogen-activated protein kinase (MAPK), and phospholipase C (PLC)-γ1 signaling *via* the TrkA receptor.[20] While the low-affinity receptor, $p75^{NTR}$, was initially known to modulate signaling through the TrkA receptor, it has become increasingly evident that NGF binding to $p75^{NTR}$ mediates its own distinct signaling pathways and cellular events, such as activation of Rac GTPase and c-Jun N-terminal kinase (JNK) signaling in mouse oligodendrocytes.[21] $p75^{NTR}$ mediates a wide range of cellular outcomes, predominantly in the nervous system. The best-known function of $p75^{NTR}$ is to mediate apoptosis during neuronal development and in response to nervous system injury.[22] In addition, $p75^{NTR}$ has been demonstrated to be involved in cell proliferation and differentiation in peripheral tissues.[23-26] However, information on the involvement and molecular insight of $p75^{NTR}$ in bone formation is limited.

Therapeutic applications of DMSCs rely on manipulating the intricate mechanisms that govern the fate and delineation of these multipotent cells. Among many levels of control, recent studies have identified the epigenetic component, including histone modifications and DNA methylation, as a key regulator in the lineage-specific differentiation of MSCs.[27-29] Epigenetics shapes cell fate determination through heritable modifications in the chromatic architecture and the accessibility of genes without changing the primary nucleotide sequence. Epigenetic phenomena are largely responsible for the elaborate orchestration of gene activation and inhibition at specific time points, directed towards the terminally differentiated phenotype of MSCs.[30,31] Nonetheless, mechanistic insight into the regulation of NGF-mediated osteogenic differentiation in DMSCs, including epigenetics, is largely unknown.

In this study, we examined the involvement of specific signaling pathways and epigenetics in NGF-induced DMSC osteogenic commitment as elucidating the detailed molecular mechanisms of NGF's effects on DMSCs may hold the key to advancing the clinical success of craniofacial bone regeneration. We discovered that NGF selectively induced the expression of Lysine Demethylase 4B (KDM4B), which is an essential player in MSC osteogenic and chondrogenic fate determination,[32,33] through JNK signaling. KDM4B directly and epigenetically activates DLX5 (Distal-Less Homeobox 5), a master osteogenic gene, by demethylating H3K9me3 marks.

Materials and Methods

Cell Isolation, Culture, and Treatment

Primary human DMSCs were isolated from 4 different donors' craniofacial tissues (IRB#13-000241) including 2 males and 2 females aged from 17 to 24 years old. Human BMSCs were purchased from ATCC (PCS-500-012; VA, USA). Cells were grown in alpha-modified Eagle's medium supplemented with 15% fetal bovine serum (Thermo Fisher Scientific, MA, USA catalog no. 26140-079) in a humidified 5% CO_2 incubator at 37°C. The osteogenic inducing medium (OIM) consisted of MEMα supplemented with 10% FBS (Thermo Fisher Scientific, catalog no. 26140-079), 10 nM dexamethasone (Sigma–Aldrich, MO, USA, catalog no. D4902), 100 μM

ascorbic acid (Sigma–Aldrich, catalog no. A4403) and 2 mM β-glycerophosphate (Sigma–Aldrich, catalog no. G9422) with or without NGF (2 or 10 ng/mL) (R&D Systems, MN, USA, catalog no. 256-GF-100/CF). The media was changed every 2 days. For JNK inhibitor (JNKi) (SP600125; Santa Cruz Biotechnology, TX, USA, catalog no. sc-200635) treatment, cells were pretreated with JNKi (5 or 10 μM) for 2 h and then treated with NGF and JNKi.

Viral Infection

For viral infection, DMSCs were plated overnight and then infected with lentiviruses with polybrene (6 μg/mL, Sigma–Aldrich, catalog no. H9268) for 24 h. The efficiency of knockdown was confirmed by quantitative real-time-PCR (qRT-PCR) and Western blot. The target sequence for shRNA was as follow: shKDM4B 5′-CCTGCCTCTAGGTTCATAA-3′.

siRNA-Mediated Knockdown

siRNA pools targeting $p75^{NTR}$, KDM4B, and c-Jun were purchased from Santa Cruz Biotechnology. DMSCs were transfected with siRNAs using Lipofectamine® 2000 Transfection Reagent (Thermo Fisher Scientific). Forty-eight hours after transfection, knockdown efficiencies were determined by qRT-PCR or Western blot. siRNAs used in this study were: $p75^{NTR}$ siRNA ID: sc-36058; KDM4B siRNA ID: sc-62517; c-Jun siRNA ID: sc-29223. For cell functional analyses, DMSCs were pretreated with siRNAs for 2 days and then changed to a new medium.

Alkaline Phosphatase Analysis

For alkaline phosphatase (ALP) staining, cells were induced for 5 days in OIM. After fixing the cells with 70% ethanol for 10 min, the cells were stained with 0.25% naphthol AS-BI phosphate (Sigma–Aldrich, catalog no. N6125) and 0.75% Fast Blue BB (Sigma–Aldrich, catalog no. D9805) mixed solution in 0.1 M Tris buffer (pH 9.6). An ALP activity assay was performed using an equal mixture of alkaline buffer solution (Sigma–Aldrich, catalog no. A9226) and alkaline phosphate substrate solution (Sigma–Aldrich, catalog no. P7998) for 30 min at 37°C. The absorbance of the reactions was read at 405 nm and normalized based on protein concentrations.

Alizarin Red S Staining

To detect mineralization, cells were induced for 14 days in OIM. After fixing the cells with 70% ethanol for 1 h, the cells were stained with 1% Alizarin Red S (ARS; Sigma-Aldrich, catalog no. A5533) for 30 min. To quantify calcium mineral deposition, the stained area was dissolved using 10% cetylpyridinium chloride in 10 mM sodium phosphate for 30 min at room temperature. The concentration was determined by absorbance measurements at 562 nm using a microplate reader and calculated by a standard calcium curve in the same solution. The final calcium level was normalized with the total protein concentrations in each group prepared from a duplicate plate.

Quantitative Real Time-Polymerase Chain Reaction (qRT-PCR) Analysis

Total RNA was isolated from DMSCs using Trizol reagents (Thermo Fisher Scientific, catalog no. 15596018). RNAs were synthesized from cDNA with random hexamers and reverse transcriptase according to the manufacturer's protocol (New England Biolabs, MA, USA, catalog no. E6300). The qRT-PCR reactions were performed using the SYBR Green PCR kit (New England Biolabs, catalog no. E3005) and the CFX qRT-PCR Detection System. Primer sequences used are indicated in Supplementary Table S1. To calculate the relative transcriptional expression, the Ct values of interested genes were normalized by average Ct values of glyceraldehyde 3-phosphate dehydrogenase (GAPDH) as ΔCt, and fold change in the relative transcriptional expression of interested genes was indicated with $2^{-\Delta\Delta Ct}$.

Protein Extraction and Western Blot

Cells were collected into a RIPA solution with protein inhibitors. Equal amounts of protein were separated by SDS-PAGE and detected for target proteins. The protein bands were visualized by the enhanced chemo-luminescence assay (GE Healthcare, Buckinghamshire, UK) following the manufacturer's instructions and scanned by a densitometer. Antibodies used were anti-KDM4B (Cell Signaling Technology, MA, USA, catalog no. 8639), anti-JNK (Cell Signaling Technology, catalog no. 9252S), anti-phospho-JNK (Cell Signaling Technology, catalog no. 4668S), anti-c-Jun (Cell Signaling Technology, catalog no. 9165), anti-phospho-c-Jun (Cell Signaling Technology, catalog no. 3270), anti-β-catenin (Cell Signaling Technology, catalog no. 9562), anti-non-phospho (Active) β-catenin (Cell Signaling Technology, catalog no. 8814), anti-p65 (Cell Signaling Technology, catalog no. 6956), and anti-phospho-p65 (Cell Signaling Technology, catalog no. 3033).

Chromatin Immunoprecipitation (ChIP) Assays

For ChIP reaction, DMSCs were treated in a basal medium with 10 μg/mL NGF. After 2–4 h, 2×10^6 cells per group were incubated with 5 mM dimethyl 3,3′ dithiobispropionimidate-HCl (DTBP) solution (Pierce Biotechnology, MA, USA, catalog no. 20665) for 10 min in a dark area at room temperature and treated 1% formaldehyde for 15 min at 37°C. Total cell lysates were sonicated into 200–500 bp DNA fragments. Chromatin complexes were immunoprecipitated with the related antibodies and Dynabeads Protein A/G (Thermo Fisher Scientific, catalog no. 10002D/10004D). For re-ChIP assay, chromatin complexes were immunoprecipitated with c-Jun antibody first, then immunoprecipitated with KDM4B and IgG antibodies. All precipitated samples were quantified using qPCR. Data were expressed as a percentage of input DNA. Antibodies used for ChIP assays were purchased from the following commercial sources: anti-KDM4B (Abcam, MA, USA, catalog no. ab191434), anti-H3K9me3 (MilliporeSigma, MA, USA, catalog no. 8898), and anti-c-JUN (Abcam, catalog no. ab31419). Primer sequences used are indicated in Supplementary Table S1.

Scaffold Preparation

Apatite-coated poly (lactic-co-glycolic acid) (Ap-PLGA) scaffolds were prepared through solvent casting and particulate leaching process following an established protocol as previously described.[34,35] Briefly, PLGA/$CHCl_3$ solution was mixed with sucrose (200-300 μm in diameter) to achieve a porosity of 92% (v/v), and the slurry was compressed into Teflon molds. After being lyophilized overnight, the scaffolds were immersed in Milli-Q water to leach out sucrose. The scaffolds were then sterilized in 70% ethanol for 30 min and rinsed with sterile water. Last, the scaffold sheets were shaped into round discs (3 mm in diameter and

0.5 mm in height) with a biopsy punch. The PLGA scaffolds were further coated with apatite layers by incubating scaffolds in simulated body fluid (SBF). The scaffold discs were subjected to glow discharge argon plasma etching (Harrick Scientific, Pleasantville, NY). The etched scaffolds were incubated in SBF1, composed of $CaCl_2$, $MgCl_2 \bullet 6H_2O$, $NaHCO_3$, $K_2HPO_4 \bullet 3H_2O$, Na_2SO_4, KCl, and NaCl, for 24 h and then further incubated in SBF2 composed of $CaCl_2$, $K_2HPO_4 \bullet 3H_2O$, KCl, and NaCl for another 24 h at 37°C. The Ap-PLGA scaffolds were loaded with phosphate-buffered saline (PBS) or NGF (10, 50, and 250 μg/mL) and were lyophilized for further usage.

Animals and Surgical Implantation

The animal protocol for this study was approved by the Animal Research Committee at the University of California, Los Angeles. Eight-week-old male SCID mice (Charles River Laboratories, NC, USA) were randomly divided into groups (5 mice per group). Experimental mice were maintained in a specific pathogen-free animal facility 12-h light/dark cycle with free access to standard chow pellets and water *ad libitum*. Calvarial defects were created on the parietal bone with a trephine drill (3-mm-diameter). After gently removing the circular bone plug, DMSC (1×10^6 cells) was seeded with different doses (10, 50, and 250 μg/mL) of NGF scaffold as well as DMSC/Scrsh (scrambled shRNA) or DMSC/shKDM4B (1×10^6 cells)-seeded with or without 250 μg/mL NGF scaffold was placed on the defect. All mice were euthanized 8 weeks after the implantation.

Micro-computerized Tomography (Micro-CT) Analysis

The fixed calvaria was subjected to μCT scanning (SkyScan 1275; Bruker-microCT, Kontich, Belgium) using a voxel size of 10 μm^3 and a 1 mm aluminum filter at 60 kV and 166 μA. Two-dimensional slices were combined using NRecon and CTAn/CTVol programs (Bruker) to form a three-dimensional reconstruction. The region of interest (ROI) was outlined with a circular shape on consecutive transaxial sections to create a uniform volume of interest (VOI). Bone Volume/Tissue Volume (BV/TV) values were quantified using the DataViewer program (Bruker).

Histological Analysis

Decalcified tissues were cut into 5 μm sections and stained with H&E by the Tissue Procurement Core Lab (TPCL) at the University of California, Los Angeles.

Statistical Analysis

All graphs were created using GraphPad Prism software, and differences in measured variables between two groups were assessed by two-tailed Student's *t*-tests. For multiple comparisons, one-way ANOVA with Tukey's post hoc test was applied when there were more than 2 groups. A two-way ANOVA with Bonferroni post hoc test was applied when there were multiple groups across different points. When normal data distribution could not be assured, the Wilcoxon/Mann–Whitney test was applied. A *P*-value of less than .05 was considered significant. Error bars represent mean ± SEM.

Results

Nerve Growth Factor Induces Osteogenic Differentiation *via* $p75^{NTR}$ in DMSCs

To confirm the role of NGF in DMSC osteogenic differentiation, we first induced the cells to undergo osteogenic differentiation following NGF treatment. In the presence of NGF, osteogenesis of DMSCs was significantly enhanced, as demonstrated by an increase in both ALP activity after NGF treatment for 5 days and mineralization potential marked by Alizarin Red S staining (ARS) after NGF treatment for 14 days (Fig. 1A). At the molecular level, NGF also induced the expression of osteogenic marker genes including distal-less homeobox 5 (*DLX5*), RUNX family transcription factor 2 (*RUNX2*), integrin-binding sialoprotein (*IBSP*), osteocalcin (*OCN*), and osteopontin (*OPN*) after NGF treatment for 4 days in a dose-dependent manner (Fig. 1B). In examining the role of NGF in BMSCs, another adult MSC type, we found the application of NGF similarly improved the osteogenic capacity of BMSCs as determined by ARS (Supplemental Fig. S1). Next, we further investigated whether $p75^{NTR}$ has a functional link to DMSC osteogenic fate determination by genetically modulating $p75^{NTR}$. $p75^{NTR}$ was knocked down by siRNAs in DMSCs and $p75^{NTR}$ depletion was confirmed by qRT-PCR (Fig. 1C). Without $p75^{NTR}$ in DMSC/sip75^{NTR} cells, NGF was unsuccessful in promoting osteogenic differentiation, as demonstrated by a significant decrease in ALP activity and mineralization capacity (Fig. 1D, 1E). Consistent with the knockdown results using siRNAs, treatment with a $p75^{NTR}$-specific inhibitor (RO: RO082750) eliminated the NGF-induced mineralization in DMSCs as demonstrated by ARS (Fig. 1F).

KDM4B Is Required for NGF-Induced Osteogenesis

To investigate the potential roles of epigenetic modulators in NGF-induced MSC osteogenesis, we profiled the expression of histone modifiers in DMSCs following NGF treatment. The qRT-PCR results revealed that *KDM4B* was upregulated most significantly by NGF (Fig. 2A). Western blot assay confirmed that KDM4B was significantly induced by NGF treatment at the protein level (Fig. 2B). Next, we examined whether KDM4B played an essential role in the NGF-dependent osteogenic lineage commitment of DMSCs. We knocked down KDM4B by using siRNA, which resulted in the depletion of *KDM4B* in DMSCs confirmed by qRT-PCR (Fig. 2C). When *KDM4B*-depleted cells were induced to undergo osteogenic differentiation in the presence of NGF for 5 days, ALP activity of differentiating DMSCs was significantly inhibited by *KDM4B* knockdown (Fig. 2D). In addition, *KDM4B* depletion also markedly suppressed the formation of mineralized nodules after prolonged treatment with OIM for 14 days (Fig. 2E). To confirm that *KDM4B* depletion inhibited NGF-mediated osteogenic differentiation of DMSCs, we assessed the expression of osteogenic marker genes, *DLX5*, *RUNX2*, and *OCN*, after 4 days of osteogenic induction. *KDM4B*-depleted cells showed a significant reduction of all three NGF-induced osteogenic markers (Fig. 2F).

KDM4B Epigenetically Regulates *DLX5* Gene Expression by Demethylating H3K9me3 Marks

DLX5 is an essential regulator of endochondral ossification and a direct regulator of osteogenesis and osteoblast differentiation through its promotion of *OCN* gene expression.[36,37]

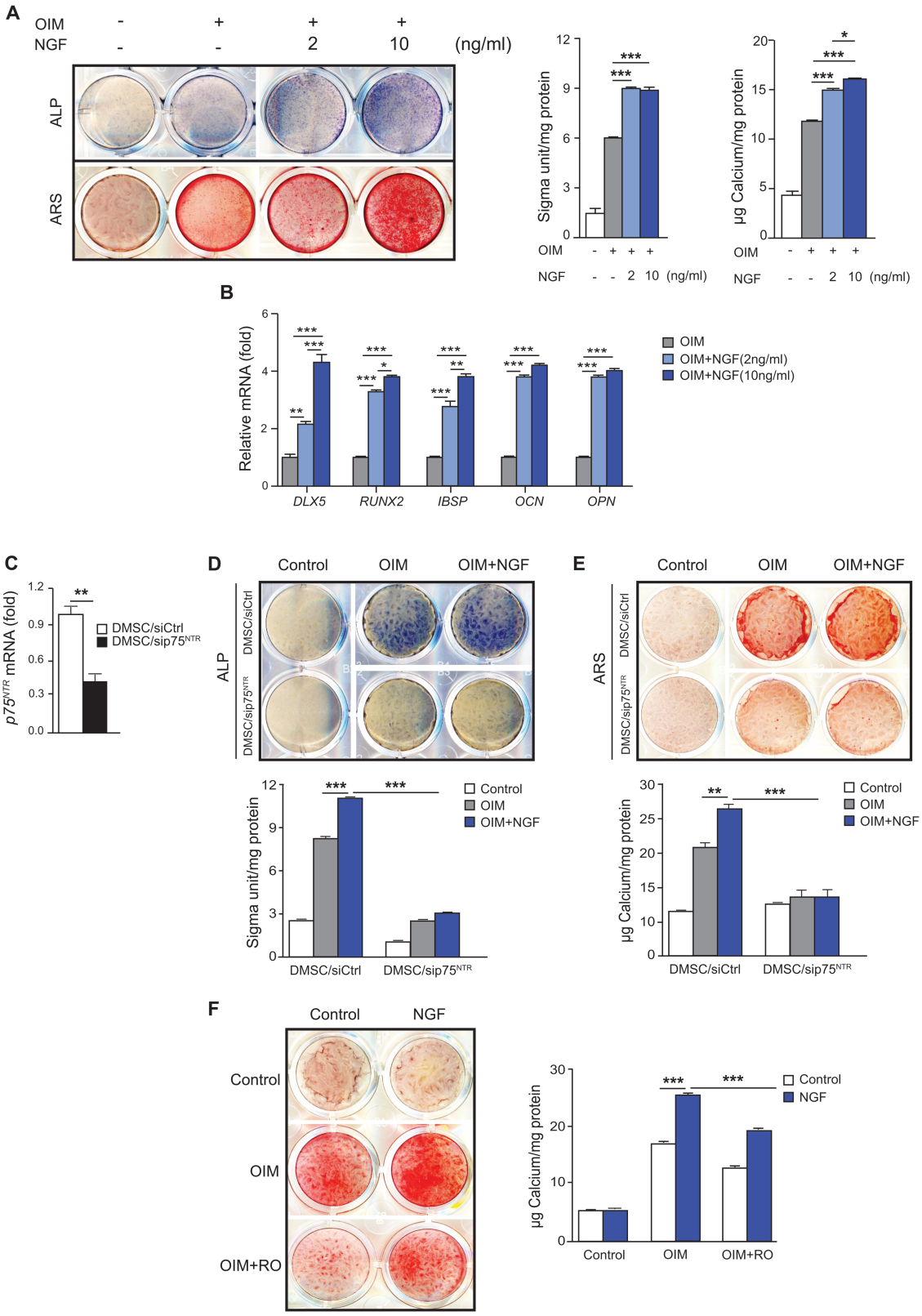

Figure 1. Nerve growth factor increases osteogenic differentiation through p75^{NTR} in DMSCs. (**A**) Alkaline phosphatase (ALP) staining and quantification after 5 days treatment and Alizarin red S (ARS) staining and quantification after 14 days treatment in osteogenic media with increasing concentrations of NGF (0, 2, 10 ng/mL). (**B**) qRT-PCR of osteogenic genes (*DLX5, RUNX2, IBSP, OCN, OPN*) after 4 days treatment in osteogenic media with varying concentrations of NGF (0, 2, 10 ng/mL). (**C**) Depletion of p75^{NTR} in DMSCs *via* siRNA by qRT-PCR. (**D**) ALP staining and quantification of p75^{NTR}-depleted DMSCs after 5 days in osteogenic media with and without 10 ng/mL NGF. (**E**) ARS staining and quantification of p75^{NTR}-depleted DMSCs after 14 days in osteogenic media with and without 10 ng/mL NGF. (**F**) ARS staining and quantification of DMSCs after 14 days in osteogenic media with and without 10 ng/mL NGF combination with 1 µM RO (RO082750). Data are presented as means ± SEMs ($n = 3$). For B and C, data are shown as fold expression of target genes after normalization to control. For A and B, the groups with different concentration of NGF were compared by one-way ANOVA with Tukey's post hoc test. For C, DMSC/siCtrl and DMSC/sip75^{NTR} were compared by two-tailed *t*-test. For D–F, all the groups were compared by two-way ANOVA with Bonferroni post hoc test. Asterisks were assigned to *P* values with statistical significances (* $P < .05$; ** $P < .01$; *** $P < .001$).

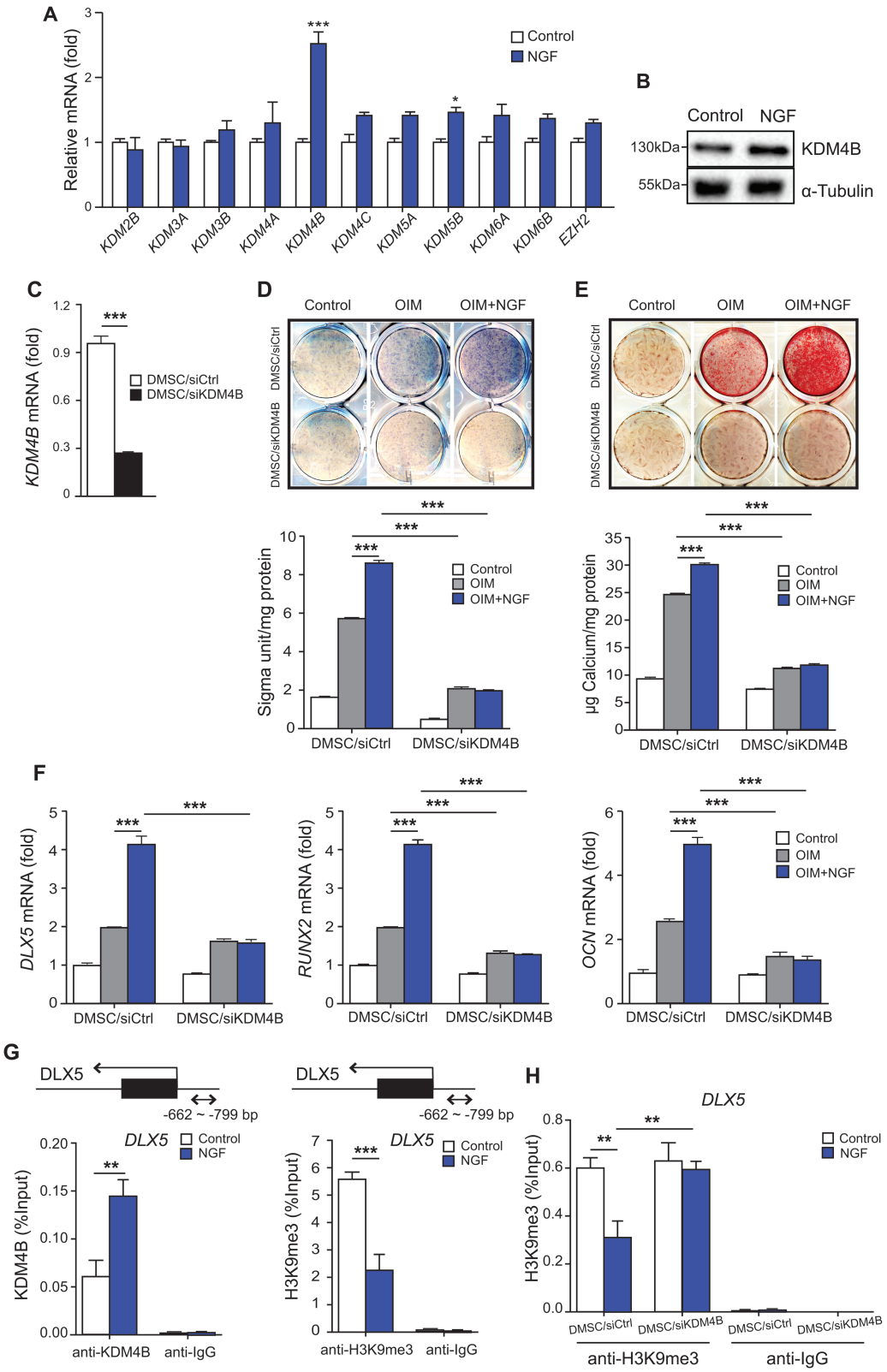

Figure 2. KDM4B is induced and critical for NGF-mediated osteogenic differentiation of DMSCs. (**A**) qRT-PCR of epigenetic genes upon NGF treatment at 2 h. Glyceraldehyde 3-phosphate dehydrogenase (GAPDH) served as an internal control. (**B**) Western blot of KDM4B and α-tubulin upon NGF treatment at 24 h. (**C**) Depletion of KDM4B in DMSCs *via* siRNA by qRT-PCR. (**D**) Alkaline phosphatase staining and quantification of KDM4B-depleted DMSCs after 5 days in osteogenic media with and without NGF. (**E**) Alizarin red S staining and quantification of KDM4B-depleted DMSCs after 14 days in osteogenic media with and without NGF. (**F**) Expression of osteogenic genes (*DLX5, RUNX2, OCN*) in KDM4B-depleted DMSCs following osteogenic induction with and without NGF for 4 d. (**G**) Occupancy of KDM4B and occupancy of H3K9me3 at DLX5 promoter, as determined by ChIP, upon NGF treatment at 2 h. (**H**) Occupancy of H3K9me3 at *DLX5* promoter in KDM4B-depleted DMSCs, as determined by ChIP, upon NGF treatment at 2 h. NGF concentration for stimulation, 10 ng/mL. Data are presented as means ± SEMs ($n = 3$). For F, data are shown as fold expression of target genes after normalization to control. For A, control and NGF treated cells were compared by two-tailed *t*-test. For C, DMSC/siCtrl and DMSC/siKDM4B were compared by two-tailed *t*-test. For D–H, all the groups were compared by two-way ANOVA with Bonferroni post hoc test. Asterisks were assigned to *P* values with statistical significances (**$P < .01$; ***$P < .001$).

In addition, DLX5 plays a role in the osteogenesis of MSCs through upregulation of the *RUNX2* gene by modulating the expression of osteogenesis-specific markers.[38,39] As NGF treatment strongly induced *DLX5* expression and such induction was inhibited by *KDM4B* depletion during DMSC osteogenesis, we examined whether KDM4B directly regulated DMSC differentiation by demethylating H3K9me3 silencing marks at the *DLX5* promoter regions. We performed ChIP assays to assess the physical occupancy of KDM4B and changes in histone methylation status at the *DLX5* promoter regions following NGF treatment. Indeed, we noticed that NGF stimulation leads to increased recruitment of KDM4B to the promoter regions of *DLX5* while H3K9me3 enrichment at the *DLX5* promoter was markedly diminished (Fig. 2G). In cells depleted of *KDM4B*, however, no significant reduction of H3K9me3 at the *DLX5* promoter region was observed following NGF induction (Fig. 2H), consistent with reduced *DLX5* mRNA in DMSC/siKDM4B cells (Fig. 2F).

JNK Signaling Pathway Mediates NGF-Induced *KDM4B* and *DLX5* Expression During NGF-Induced Osteogenic Differentiation of DMSCs

Unlike the well-characterized NGF signaling cascades through the TrkA receptor, NGF signaling pathways through $p75^{NTR}$ are less understood. NGF/$p75^{NTR}$ signaling has been reported to involve the activation of NF-κB, JNK, and β-catenin signaling pathways in different cells.[40-42] To elucidate which intracellular signaling pathways are critical in NGF-mediated MSC differentiation, we treated DMSCs with NGF (10 ng/mL) and screened for JNK, NFκB, and β-catenin pathways by Western blot. Interestingly, both phosphorylated JNK (p-JNK) and phosphorylated c-Jun (p-c-Jun) were markedly induced by NGF, while phosphorylated p65 and active β-catenin levels were slightly increased in response to NGF stimulation. These results suggest the involvement of sequential phosphorylation in the JNK-c-Jun cascade during the NGF-mediated osteogenesis of DMSCs (Fig. 3A). To further examine the involvement of the JNK pathway in NGF-induced osteogenic differentiation, we impeded JNK signaling using a pharmacological inhibitor, SP600125, in varying doses (5 μM and 10 μM). This treatment with JNKi eliminated the NGF-induced upregulation of p-JNK and p-c-Jun in a dose-dependent manner 30 min after NGF treatment (Fig. 3B). When JNK signal transduction was blocked by JNKi, NGF failed to enhance the osteogenic potential of DMSCs as demonstrated by ALP activity after NGF treatment for 5 days and mineralization potential after treatment for 14 days (Fig. 3C). These JNKi-treated DMSCs also revealed significant suppression of osteogenic marker genes, *DLX5, RUNX2, OSX,* and *OCN* (Fig. 3D), suggesting that the JNK signaling pathway is required for NGF-mediated osteogenic differentiation. Lastly, we examined the involvement of JNK signaling in the epigenetic regulation of NGF-mediated osteogenesis. Interestingly, NGF-mediated KDM4B upregulation was completely abolished following JNKi treatment, indicating that KDM4B may be controlled by the JNK pathway (Fig. 3E). Consistently, JNK inhibition attenuated KDM4B recruitment to the target gene in response to NGF stimulation (Fig. 3F). The diminished binding of KDM4B led to increased enrichment of its substrate, H3K9me3, at the *DLX5* promoter region (Fig. 3G).

c-Jun and KDM4B Work in Concert to Regulate NGF-Mediated Osteogenic Differentiation Through Simultaneous Recruitment Onto the *DLX5* Promoter

We evaluated whether a transcription factor downstream of the JNK pathway, c-Jun, directly regulates osteogenic genes during NGF-induced osteogenic differentiation. Using ChIP assays, we observed that c-Jun binds to the *DLX5* promoter in response to NGF stimulation (Fig. 4A). Conversely, when the JNK cascade was blocked by JNKi, NGF-mediated c-Jun recruitment to the *DLX5* promoter was significantly reduced (Fig. 4B). To further elucidate whether NGF-activated JNK signaling directly regulates *KDM4B* expression, we performed additional ChIP assays to assess the recruitment of c-Jun to the promoter region of *KDM4B* upon NGF treatment. We confirmed that NGF substantially enhanced the binding of c-Jun to the *KDM4B* promoter (Fig. 4C), suggesting the importance of c-Jun-dependent *KDM4B* gene expression during NGF-induced osteogenesis. These results affirm that JNK signaling induces DLX5 and KDM4B expression through the recruitment of c-Jun to target genes during NGF-mediated osteogenic differentiation. To further our understanding of the dynamics between c-Jun and KDM4B, we first knocked down c-Jun by using siRNAs to deplete transcription as confirmed by qRT-PCR (Fig. 4D). When c-Jun-depleted DMSCs were treated with NGF, we observed significantly attenuated KDM4B induction by NGF (Fig. 4E). After discovering that both KDM4B and c-Jun bind to the *DLX5* promoter region in response to NGF stimulation (Figs. 2G and 4A), we sought to elucidate the recruitment hierarchy of c-Jun and KDM4B to the *DLX5* promoter region. First, we assessed KDM4B physical occupancy at the *DLX5* promoter in c-Jun depleted DMSCs. Enhanced KDM4B recruitment to the *DLX5* promoter region in response to NGF stimulation was significantly suppressed in the absence of c-Jun (Fig. 4F, Left). As expected, increased H3K9me3 removal by NGF-induced KDM4B present at the *DLX5* promoter region was inhibited in sic-Jun-treated DMSCs (DMSC/sic-Jun) compared to control siRNA-treated DMSCs (DMSC/siCtrl) (Fig. 4F, Right). These results suggest that KDM4B binding to the *DLX5* promoter and subsequent epigenetic regulation of *DLX5* gene activation is dependent on c-Jun. Next, we knocked down *KDM4B* using siKDM4B in DMSCs to evaluate c-Jun recruitment to the *DLX5* promoter in these cells. Notably, we observed that as with JNK inhibition, depletion of *KDM4B* obliterated NGF-dependent recruitment of c-Jun to the *DLX5* promoter (Fig. 4G), disabling c-Jun mediated *DLX5* transcription. These results indicate that the interdependent recruitment of c-Jun and KDM4B to the *DLX5* promoter is required for NGF-mediated DMSC osteogenic differentiation. To determine the association between c-Jun and KDM4B at the *DLX5* promoter, we used sequential ChIP (re-ChIP) assays. For the first ChIP, antibodies to c-Jun and IgG were used and for the second ChIP, antibodies to KDM4B and IgG were used. The re-ChIP assay determined by qPCR showed that both c-Jun and KDM4B could simultaneously co-occupy the same region of the *DLX5* promoter (Fig. 4H). These data suggest that the enhancement of *DLX5* promoter activity relies on the binding of the c-Jun/KDM4B complex to the promoter region of *DLX5*.

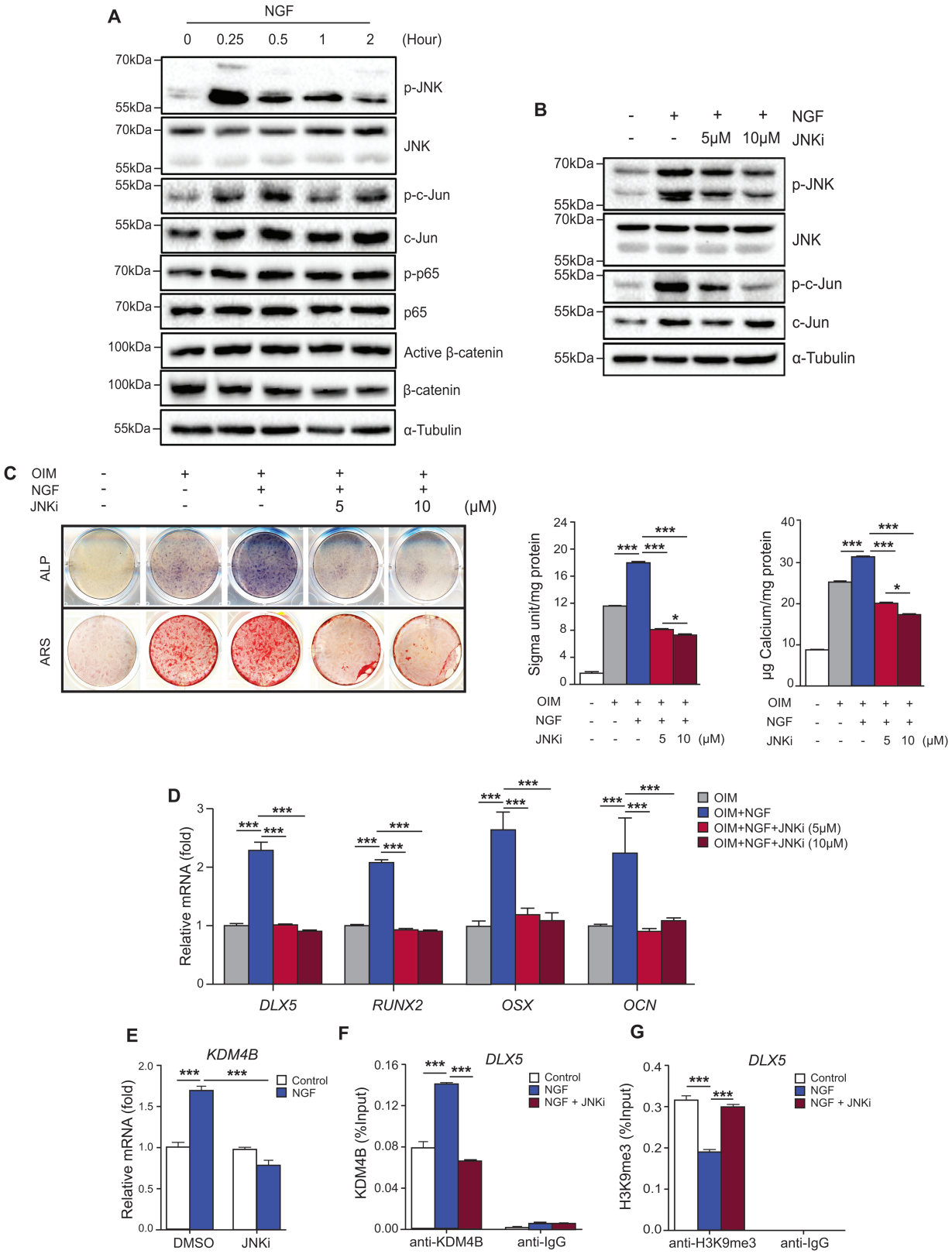

Figure 3. JNK signaling pathway is involved in NGF-mediated KDM4B expression in DMSCs. (**A**) Western blot of JNK signaling pathway (phospho-JNK, JNK, phospho-c-Jun, c-Jun), total and phospho-p65, total and active β-catenin and α-Tubulin upon NGF treatment at different time points (0, 0.25, 0.5, 1, 2 h). (**B**) Western blot of JNK signaling pathway (p-JNK, JNK, p-c-Jun, c-Jun, α-tubulin) pretreated with 5 μM or 10 μM JNKi (JNK inhibitor) at 2 h upon NGF treatment. (**C**) Alkaline phosphatase staining and quantification after 5 days treatment and Alizarin red S staining and quantification after 14 days treatment in osteogenic media with pretreated different doses of JNKi (5 μM and 10 μM) upon NGF treatment. (**D**) Expression of osteogenic genes (DLX5, RUNX2, OSX, OCN) pretreated with 10 μM JNKi at 2 h upon osteogenic media with NGF for 4 days in DMSCs. (**E**) Gene expression of KDM4B pretreated with 10 μM JNKi at 2 h upon NGF treatment. (**F**) Occupancy of KDM4B at DLX5 promoter as determined by ChIP, pretreated with 10 μM JNKi at 2 hours upon NGF treatment. (**G**) Occupancy of H3K9me3 at DLX5 promoter as determined by ChIP, pretreated with 10 μM JNKi at 2 h upon NGF treatment. NGF concentration for stimulation, 10 ng/mL. Data are presented as means ± SEMs ($n = 3$). For D, data are shown as fold expression of target genes after normalization to control. For C and D, all groups were compared by one-way ANOVA with Tukey's post hoc test. For E–G, all the groups were compared by two-way ANOVA with Bonferroni post hoc test. Asterisks were assigned to P values with statistical significances (*$P < .05$; ***$P < .001$).

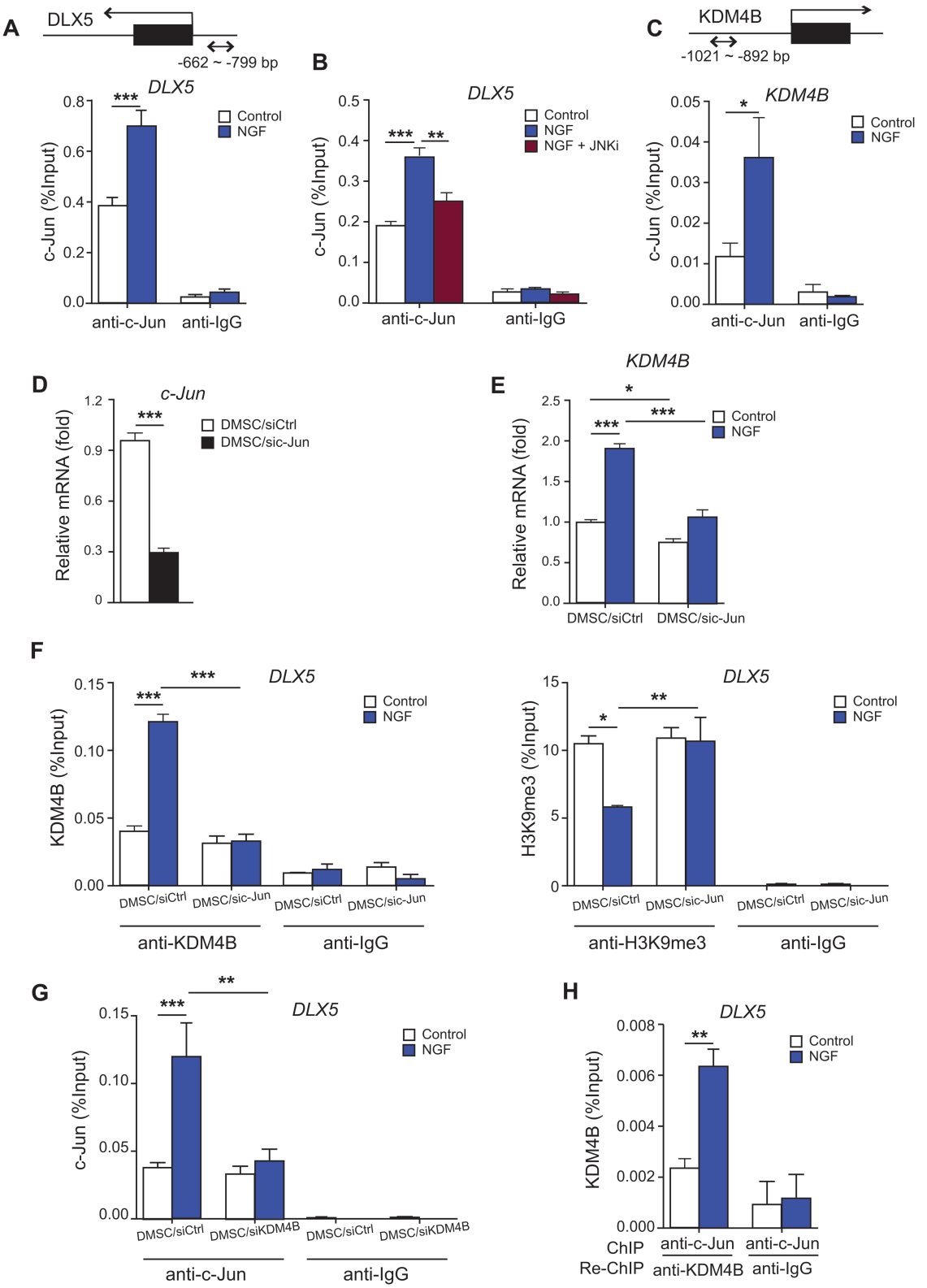

Figure 4. Co-occupancy of c-Jun and KDM4B occurs at *DLX5* promoter. (**A**) Occupancy of c-Jun at *DLX5* promoter, as determined by ChIP, upon NGF treatment. (**B**) Occupancy of c-Jun at DLX5 promoter as determined by ChIP, pretreated with 10 μM JNKi at 2 h upon NGF treatment. (**C**) Occupancy of c-Jun at KDM4B promoter, as determined by ChIP, upon NGF treatment. (**D**) Depletion of c-Jun in DMSCs *via* siRNA by qRT-PCR. (**E**) Gene expression of KDM4B in control and c-Jun-depleted DMSCs upon NGF treatment. (**F**) Occupancy of KDM4B (Left) and H3K9me3 (Right) at *DLX5* promoter in c-Jun-depleted DMSCs, as determined by ChIP, upon NGF treatment. (**G**) Occupancy of c-Jun at *DLX5* promoter in KDM4B-depleted DMSCs, as determined by ChIP, upon NGF treatment. (**H**) Co-occupancy of c-JUN and KDM4B at *DLX5* promoter by the Re-ChIP assay, upon NGF treatment. NGF concentration for stimulation, 10 ng/ml. Data are presented as means ± SEMs ($n = 3$). For D and E, data are shown as fold expression of target genes after normalization to DMSC/siCtrl. For D, DMSC/siCtrl and DMSC/sic-Jun were compared by two-tailed *t*-test. For A–H except D, all the groups were compared by two-way ANOVA with Bonferroni post hoc test. Asterisks were assigned to *P* values with statistical significances (*$P < .05$; **$P < .01$; ***$P < .001$).

KDM4B is Required for NGF-Mediated DMSC Bone Formation in vivo

To assess the ability of NGF to promote bone regeneration in mice, critical-sized calvarial defects were generated in 8-week-old SCID mice. Ap-PLGA scaffolds were loaded with various concentrations of NGF (0, 10, 50, and 250 μg/mL) and implanted into the defects. Micro-CT images demonstrated maximum bone formation at 50 and 250 μg/mL NGF compared to the scaffold without NGF loading (Supplemental Fig. S2A). Quantitative analysis of micro-CT images was performed by calculating bone volume/tissue volume (BV/TV). Results revealed that defects with control scaffolds only showed minimal bone healing of 12.56 ± 1.91% (BV/TV) after 8 weeks. In contrast, calvarial defects treated with varying doses of NGF showed significant increases in bone repair, with 23.92 ± 8.92% (BV/TV) at 50 μg/mL, and 24.67 ± 4.49% (BV/TV) at 250 μg/mL (Fig. 5A). Consistently, H&E staining showed that NGF remarkably increased new bone area in high concentrations of 50 and 250 μg/mL in vivo (Supplemental Fig. S2B, S2C). Following the 10 μg/mL NGF treatment, no increase in bone volume was seen compared to the control. There was no significant difference in bone volume between 50 μg/mL and 250 μg/mL of NGF treatment dosing. To verify our in vitro findings that suggest KDM4B plays a critical role in NGF-mediated osteogenesis, we assessed whether the knockdown of *KDM4B* affected DMSC-mediated bone regeneration in vivo using a calvarial defect mouse model. We depleted *KDM4B* by transducing cells with lentiviruses expressing *KDM4B* shRNA targeting the coding sequences of KDM4B mRNA. The efficiency of depletion of KDM4B in DMSCs was confirmed by Western blot (Fig. 5B). DMSC/Scrsh and DMSC/shKDM4B cells were seeded in the scaffolds with and without 250 μg/mL NGF and subsequently transplanted into the calvarial defects. After 8 weeks, crania with transplanted scaffolds were harvested and prepared for micro-CT and histological analysis. Visualization

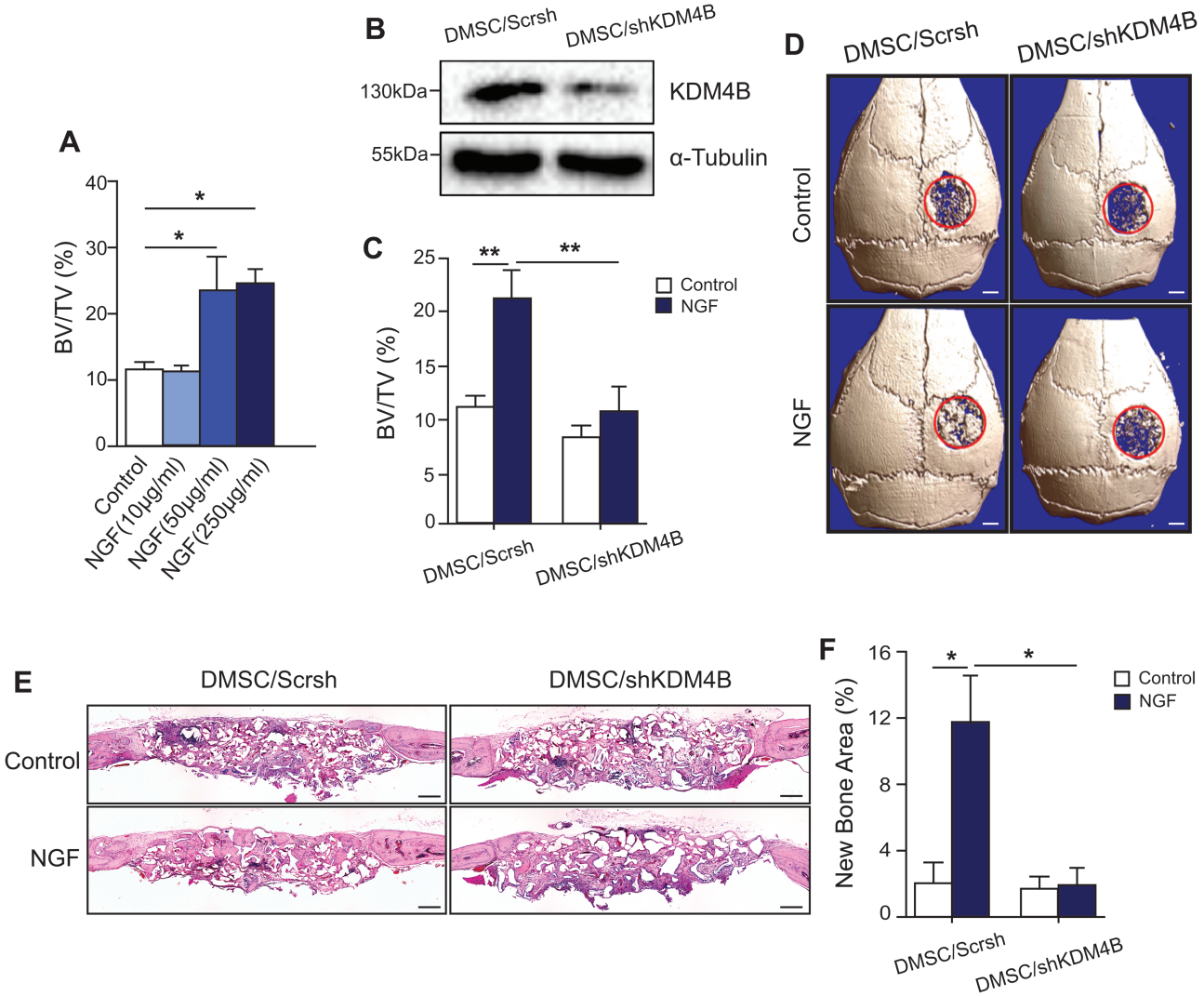

Figure 5. KDM4B is essential for NGF-mediated bone formation in vivo. (**A**) Bone volume quantification (BV/TV) of calvarial bone defects with scaffolds seeded with DMSCs containing different concentrations of NGF (0, 10, 50, 250 μg/mL). (**B**) Depletion of KDM4B in DMSCs *via* shRNA as determined by Western blot. (**C**) Bone volume quantification (BV/TV) and (**D**) 3D Micro-CT images of calvarial bone defects with scaffolds seeded with DMSC/shKDM4B or DMSC/Scrsh under the presence of NGF. Scale bar, 1 mm. (**E**) H&E staining images and (**F**) histomorphometric analysis for new bone area within calvarial bone defects from the mice transplanted scaffolds seeded DMSC/shKDM4B or DMSC/Scrsh in the presence of NGF. Scale bar, 25 μm. NGF concentration for stimulation, 250 μg/mL. Data presented as means ± SEMs ($n = 5$). For C and F, all the groups were compared by two-way ANOVA with Bonferroni post hoc test. Asterisks were assigned to P values with statistical significances (*$P < .05$; **$P < .01$).

and quantitative analysis of micro-CT images revealed that the NGF treatment was unable to promote bone repair in the absence of KDM4B while the defect seeded with DMSC/Scrsh cells showed significantly enhanced bone formation by NGF (Fig. 5C, 5D). Consistently, H&E staining showed that the loss of KDM4B abrogated the pro-osteogenic effects of NGF in vivo (Fig. 5E, 5F).

Discussion

The underlying objective of this study was to elucidate the molecular and epigenetic mechanistic insight of NGF-mediated DMSC osteogenesis through in vitro and in vivo experiments. Nerve growth factor was initially discovered as a growth factor, shown to promote the differentiation and maturation of sensory and sympathetic ganglia.[43] Although the NGF signaling pathway has been rigorously studied for its regulation of the peripheral nervous system to noxious stimuli, few efforts have focused on the coordinate effects of NGF, TrkA, and $p75^{NTR}$ in skeletal tissues.[16,44] In the limited number of prior studies on NGF-mediated bone regeneration, NGF was administered at very high doses to the fracture model, and osteogenic potential was assessed by monitoring neurogenesis rather than performing a comprehensive structural analysis on newly formed bone.[45,46] More recently, an elegant study demonstrated that NGF-TrkA signaling is required for stress fracture repair in a genetic model, stimulating intramembranous healing through increased peripheral nerve innervation, angiogenesis, and osteogenesis.[47] Another study revealed that osteogenically favorable conditions and mechanical stimulation increase NGF biosynthesis, activating TrkA sensory nerves and osteogenic gene transcription.[48,49] Finally, osteoblasts up-regulate NGF expression on both periosteal and endosteal ulnar surfaces, strongly suggesting that sensory nerves at these sites respond to NGF-TrkA signaling.[50] Although studies have revealed the significance of TrkA-mediated NGF signaling in bone, the exact role of $p75^{NTR}$ in this pathway remains minimally known. We have previously reported that $p75^{NTR}$ is the most effective marker for isolating DMSCs with the strongest odontogenic and chondrogenic potential.[5] Moreover, $p75^{NTR}$-positive DMSC populations exhibit the most significant upregulation of osteogenic marker genes.[51] In the present study, we demonstrated that $p75^{NTR}$ was required for the NGF-induced osteogenesis of DMSCs, indicating that $p75^{NTR}$ serves as a functional surface marker in DMSCs. According to recent studies, deletion of $p75^{NTR}$ reduces alveolar bone mass and dental hard tissue formation in mice as well as the osteogenic differentiation of ectomesenchymal stem cells (EMSCs).[52,53] This is consistent with a previous study demonstrating that the deletion of $p75^{NTR}$ for blocking tumor necrosis factor-alpha signaling impairs bone regeneration during bone repair in mice.[54]

Epigenetic modifications, such as histone methylation, lead to functionally relevant alterations in the genome without any changes in the nucleotide sequence.[55] Our group first reported that KDM4B is an essential player in MSC osteogenic and chondrogenic fate determination by removing H3K9me3 epigenetic marks.[32,33] Our previous microarray analysis indicated that KDM4B globally controls the expression of genes associated with osteoblast differentiation and bone development.[32] Our recent study also showed that KDM4B deletion impaired MSC self-renewal and parathyroid hormone-mediated MSC osteogenic differentiation.[56] Using *Kdm4b* knockout mice, we also uncovered that the loss of KDM4B in MSCs exacerbates bone loss and skeletal aging by suppressing bone formation and increasing bone marrow adipose tissue.[56] Interestingly, a recent study by Yi et al. demonstrated that KDM4B is also crucial for osteoclastogenesis through KDM4B-CCAR1-MED1 signaling, suggesting that NGF-activated KDM4B potentially functions at multiple fronts to enhance osteogenic differentiation and bone formation in vivo.[57] Although KDM4B's importance in bone formation has been elucidated previously, the mechanism of KDM4B in response to NGF stimulation has not been known.

DLX5 is the master osteogenic gene and one of the earliest transcription factors to determine osteo-specific cell lineage.[38] In this study, we examined KDM4B's binding to the *DLX5* promoter region as in our previous study which demonstrated KDM4B's binding to the *DLX5* promoter following BMP4/7 treatment in human BMSCs. Similarly, we observed the physical occupancy of KDM4B on the *DLX5* promoter following NGF stimulation, revealing that KDM4B directly regulated *DLX5* expression. While previous studies reported that KDM4B is capable of regulating target genes in a demethylase-independent manner,[58,59] our ChIP assays showed that KDM4B removes H3K9me3 marks at the *DLX5* promoter during NGF-induced osteogenesis. In this study, we found that inhibition of KDM4B suppressed the expression of major osteogenic transcription factors, DLX5, RUNX2, and OCN. While KDM4B's binding to osteogenic genes other than *DLX5* in human cells is not known, our previous ChIP-seq results demonstrated that KDM4B was present on the promoter of *Runx2* and that the deletion of KDM4B increased H3K9me3 enrichment on the promoter region of *Runx2* in mouse BMSCs. Therefore, KDM4B's effect on RUNX2 and OCN may be an indirect regulation through DLX5 in human cells, but it is also possible that NGF-induced KDM4B and epigenetically controls the transcriptional activation of additional genes leading to enhanced osteogenesis. Our study demonstrated that this epigenetic regulation of *DLX* expression was dependent on c-Jun as KDM4B is directly induced by NGF-activated JNK signaling and works in concert with c-Jun to mediate NGF-dependent *DLX5* activation to promote NGF's anabolic events.

In the present study, the mechanism of $p75^{NTR}$-mediated NGF signaling was examined only in DMSCs. Further investigation of this pathway in stem cells of other origins would allow for the development of a wider array of bone regenerative therapies. Moreover, we established that NGF modulates osteogenic differentiation through the removal of H3K9me3 marks by KDM4B. Additional studies focused on other epigenetic marks, such as the methylation of H3K27, may be beneficial to further elucidate the epigenetic regulation of osteogenic pathways in MSCs. Finally, additional mechanistic studies will be required to determine the specific surface receptor that NGF interacts with to induce the proposed signaling cascade. Although we proved that NGF-mediated osteogenic induction in DMSCs requires $p75^{NTR}$, it is not clear whether this occurs through direct binding of NGF to the $p75^{NTR}$ receptor or through interactions between the $p75^{NTR}$ receptor and other NGF binding surface receptors such as TrkA. Additional insight into the more specific details of this cascade would better inform efforts to develop therapies for bone regeneration.

Conclusion

Epigenetic regulation is critical to orchestrating complex gene expression patterns during stem cell differentiation and bone regeneration.[60,61] Here, for the first time, we identified KDM4B as a critical epigenetic factor that mediates NGF-induced DMSC osteogenic commitment and DMSC-mediated craniofacial regeneration in vivo. Our study revealed that NGF mediates osteogenic induction in DMSCs through the $p75^{NTR}$ receptor, with KDM4B playing an indispensable role in NGF-mediated osteogenic differentiation as a key epigenetic molecule. Mechanically, c-Jun and KDM4B work in concert to promote efficient NGF-dependent *DLX5* transcriptional activation to enhance the osteogenic commitment of DMSCs. Collectively, our data demonstrated that NGF activates the JNK signaling cascade which functions as a positive regulator of KDM4B and DLX5 during NGF-mediated bone formation as well as osteogenesis of DMSCs.

Acknowledgments

This work was supported by NIH/NIDCR grants K08DE024603, R01DE019412, R01DE028260, and R01DE024828. The content is solely the responsibility of the authors and does not necessarily represent the official views of the National Institutes of Health.

Conflict of Interest

The authors do not have any conflict of interest, financial affiliation, or involvement with any commercial organization with a direct financial interest in the subject or materials discussed in this manuscript.

Author Contributions

Z.L., J.S.S., P.D.: collection and/or assembly of data, data analysis and interpretation, manuscript writing, final approval of manuscript, visualization, and manuscript revising. O.B.: provision of study material, data analysis, and interpretation, final approval of manuscript. M.D.: manuscript writing, final approval of manuscript. M.M.: visualization, final approval of manuscript. Z.-K.C.: provision of study material, final approval of manuscript. M.L.: provision of study material, final approval of manuscript. T.A.: data analysis and interpretation, final approval of manuscript. C.-Y.W., C.H.: conception and design, financial support, administrative support, data analysis and interpretation, manuscript writing, final approval of manuscript, and manuscript revising, supervision. All authors were involved in drafting the article and approved the final version of the paper.

Data Availability

The data that support the findings of this study are available from the corresponding author upon reasonable request.

Supplementary Material

Supplementary material is available at *Stem Cells* online.

References

1. Caplan AI. Mesenchymal stem cells and gene therapy. *Clin Orthop Relat Res*. 2000;379(Suppl):S67-S70.
2. Wang F, Yu M, Yan X, et al. Gingiva-derived mesenchymal stem cell-mediated therapeutic approach for bone tissue regeneration. *Stem Cells Dev*. 2011;20(12):2093-2102.
3. Arpornmaeklong P, Brown SE, Wang Z, et al. Phenotypic characterization, osteoblastic differentiation, and bone regeneration capacity of human embryonic stem cell-derived mesenchymal stem cells. *Stem Cells Dev*. 2009;18(7):955-968.
4. Wang Z, Han L, Sun T, et al. Osteogenic and angiogenic lineage differentiated adipose-derived stem cells for bone regeneration of calvarial defects in rabbits. *J Biomed Mater Res A*. 2021;109(4):538-550.
5. Alvarez R, Lee HL, Hong C, et al. Single CD271 marker isolates mesenchymal stem cells from human dental pulp. *Int J Oral Sci*. 2015;7(4):205-212.
6. Zhang W, Walboomers XF, Shi S, et al. Multilineage differentiation potential of stem cells derived from human dental pulp after cryopreservation. *Tissue Eng*. 2006;12(10):2813-2823.
7. Fujii Y, Kawase-Koga Y, Hojo H, et al. Bone regeneration by human dental pulp stem cells using a helioxanthin derivative and cell-sheet technology. *Stem Cell Res Ther*. 2018;9(1):24.
8. d'Aquino R, De Rosa A, Lanza V, et al. Human mandible bone defect repair by the grafting of dental pulp stem/progenitor cells and collagen sponge biocomplexes. *Eur Cell Mater*. 2009;18(7):75-83.
9. Casaccia-Bonnefil P, Gu C, Chao M. Neurotrophins in cell survival/death decisions. *Adv Exp Med Biol*. 1999;468:275-282.
10. Frebel K, Wiese S. Signalling molecules essential for neuronal survival and differentiation. *Biochem Soc Trans*. 2006;34(Pt 6):1287-1290.
11. Hayashi K, Storesund T, Schreurs O, et al. Nerve growth factor beta/pro-nerve growth factor and their receptors in normal human oral mucosa. *Eur J Oral Sci*. 2007;115(5):344-354.
12. Freund V, Frossard N. Expression of nerve growth factor in the airways and its possible role in asthma. *Prog Brain Res*. 2004;146:335-346.
13. Gaspersic R, Kovacic U, Glisovic S, et al. Anti-NGF treatment reduces bone resorption in periodontitis. *J Dent Res*. 2010;89(5):515-520.
14. Maltman DJ, Hardy SA, Przyborski SA. Role of mesenchymal stem cells in neurogenesis and nervous system repair. *Neurochem Int*. 2011;59(3):347-356.
15. Hofer HR, Tuan RS. Secreted trophic factors of mesenchymal stem cells support neurovascular and musculoskeletal therapies. *Stem Cell Research & Therapy* 2016;7(1):1-14.
16. Asaumi K, Nakanishi T, Asahara H, et al. Expression of neurotrophins and their receptors (TRK) during fracture healing. *Bone*. 2000;26(6):625-633.
17. Wang L, Cao J, Lei DL, et al. Application of nerve growth factor by gel increases formation of bone in mandibular distraction osteogenesis in rabbits. *Br J Oral Maxillofac Surg*. 2010;48(7):515-519.
18. Micera A, Lambiase A, Stampachiacchiere B, et al. Nerve growth factor and tissue repair remodeling: trkANGFR and p75NTR, two receptors one fate. *Cytokine & Growth Factor Rev*. 2007;18(3-4):245-256.
19. Brunet A, Datta SR, Greenberg ME. Transcription-dependent and -independent control of neuronal survival by the PI3K–Akt signaling pathway. *Curr Opin Neurobiol*. 2001;11(3):297-305.
20. Patapoutian A, Reichardt LF. Trk receptors: mediators of neurotrophin action [in Eng]. *Curr Opin Neurobiol*. 2001;11(3):272-280.
21. Harrington AW, Kim JY, Yoon SO. Activation of Rac GTPase by p75 is necessary for c-jun N-terminal kinase-mediated apoptosis. *J Neurosci*. 2002;22(1):156-166.
22. Beattie MS, Harrington AW, Lee R, et al. ProNGF induces p75-mediated death of oligodendrocytes following spinal cord injury. *Neuron*. 2002;36(3):375-386.

23. Zhang M, Cao Y, Li X, et al. Cd271 mediates proliferation and differentiation of epidermal stem cells to support cutaneous burn wound healing. *Cell Tissue Res*. 2018;371(2):273-282.
24. Restivo G, Diener J, Cheng PF, et al. Publisher correction: the low affinity neurotrophin receptor CD271 regulates phenotype switching in melanoma. *Nat Commun*. 2018;9(1):314.
25. Calabrese G, Giuffrida R, Lo Furno D, et al. Potential effect of CD271 on human mesenchymal stromal cell proliferation and differentiation. *Int J Mol Sci*. . 2015;16(7):15609-15624.
26. Wen X, Liu L, Deng M, et al. Characterization of p75(+) ectomesenchymal stem cells from rat embryonic facial process tissue. *Biochem Biophys Res Commun*. 2012;427(1):5-10.
27. Egger G, Liang G, Aparicio A, et al. Epigenetics in human disease and prospects for epigenetic therapy. *Nature*. 2004;429(6990):457-463.
28. Ozkul Y, Galderisi U. The impact of epigenetics on mesenchymal stem cell biology. *J Cell Physiol*. 2016;231(11):2393-2401.
29. Perez-Campo FM, Riancho JA. Epigenetic mechanisms regulating mesenchymal stem cell differentiation. *Curr Genomics*. 2015;16(6):368-383.
30. Ren J, Huang D, Li R, et al. Control of mesenchymal stem cell biology by histone modifications. *Cell Biosci*. 2020;10:11.
31. Li Z, Liu C, Xie Z, et al. Epigenetic dysregulation in mesenchymal stem cell aging and spontaneous differentiation. *PLoS One*. 2011;6(6):e20526.
32. Ye L, Fan Z, Yu B, et al. Histone demethylases KDM4B and KDM6B promotes osteogenic differentiation of human MSCs. *Cell Stem Cell*. 2012;11(1):50-61.
33. Lee HL, Yu B, Deng P, et al. Transforming growth factor-beta-induced KDM4B promotes chondrogenic differentiation of human mesenchymal stem cells. *Stem Cells*. 2016;34(3):711-719.
34. Fan J, Lee CS, Kim S, et al. Trb3 controls mesenchymal stem cell lineage fate and enhances bone regeneration by scaffold-mediated local gene delivery. *Biomaterials*. 2021;264:120445.
35. Fan J, Im CS, Cui ZK, et al. Delivery of phenamil enhances BMP-2-induced osteogenic differentiation of adipose-derived stem cells and bone formation in calvarial defects. *Tissue Eng Part A*. 2015;21(13-14):2053-2065.
36. Robledo RF, Rajan L, Li X, et al. The Dlx5 and Dlx6 homeobox genes are essential for craniofacial, axial, and appendicular skeletal development. *Genes Dev*. 2002;16(9):1089-1101.
37. Hassan MQ, Tare R, Lee SH, et al. HOXA10 controls osteoblastogenesis by directly activating bone regulatory and phenotypic genes. *Mol Cell Biol*. 2007;27(9):3337-3352.
38. Lee MH, Kim YJ, Yoon WJ, et al. Dlx5 specifically regulates Runx2 type II expression by binding to homeodomain-response elements in the Runx2 distal promoter. *J Biol Chem*. 2005;280(42):35579-35587.
39. Heo JS, Lee SG, Kim HO. Distal-less homeobox 5 is a master regulator of the osteogenesis of human mesenchymal stem cells. *Int J Mol Med*. 2017;40(5):1486-1494.
40. Casaccia-Bonnefil P, Carter BD, Dobrowsky RT, et al. Death of oligodendrocytes mediated by the interaction of nerve growth factor with its receptor p75. *Nature*. 1996;383(6602):716-719.
41. Carter BD, Kaltschmidt C, Kaltschmidt B, et al. Selective activation of NF-κB by nerve growth factor through the neurotrophin receptor p75. *Science*. 1996;272(5261):542-545.
42. Li B, Cai S, Zhao Y, et al. Nerve growth factor modulates the tumor cells migration in ovarian cancer through the WNT/β-catenin pathway. *Oncotarget*. 2016;7(49):81026-81048.
43. Aloe L. Rita Levi-Montalcini: the discovery of nerve growth factor and modern neurobiology. *Trends Cell Biol*. 2004;14(7):395-399.
44. Mantyh PW, Koltzenburg M, Mendell LM, et al. Antagonism of nerve growth factor-TrkA signaling and the relief of pain. *Anesthesiology*. 2011;115(1):189-204.
45. Chen WH, Mao CQ, Zhuo LL, et al. Beta-nerve growth factor promotes neurogenesis and angiogenesis during the repair of bone defects. *Neural Regen Res*. 2015;10(7):1159-1165.
46. Grills BL, Schuijers JA, Ward AR. Topical application of nerve growth factor improves fracture healing in rats. *J Orthop Res*. 1997;15(2):235-242.
47. Li Z, Meyers CA, Chang L, et al. Fracture repair requires TrkA signaling by skeletal sensory nerves. *J Clin Invest*. 2019;129(12):5137-5150.
48. Grassel S, Ahmed N, Gottl C, et al. Gene and protein expression profile of naive and osteo-chondrogenically differentiated rat bone marrow-derived mesenchymal progenitor cells. *Int J Mol Med*. 2009;23(6):745-755.
49. Tomlinson RE, Li Z, Li Z, et al. NGF-TrkA signaling in sensory nerves is required for skeletal adaptation to mechanical loads in mice. *Proc Natl Acad Sci USA*. 2017;114(18):E3632-E3641.
50. Lara-Castillo N, Kim-Weroha NA, Kamel MA, et al. In vivo mechanical loading rapidly activates beta-catenin signaling in osteocytes through a prostaglandin mediated mechanism. *Bone*. 2015;76:58-66.
51. Alvarez R, Lee HL, Wang CY, et al. Characterization of the osteogenic potential of mesenchymal stem cells from human periodontal ligament based on cell surface markers. *Int J Oral Sci*. 2015;7(4):213-219.
52. Wang Y, Yang K, Li G, et al. p75NTR(–/–) mice exhibit an alveolar bone loss phenotype and inhibited PI3K/Akt/beta-catenin pathway. *Cell Prolif*. 2020;53(4):e12800.
53. Zhao M, Wang Y, Li G, et al. The role and potential mechanism of p75NTR in mineralization via in vivo p75NTR knockout mice and in vitro ectomesenchymal stem cells. *Cell Prolif*. 2020;53(2):e12758.
54. Gerstenfeld LC, Cho TJ, Kon T, et al. Impaired intramembranous bone formation during bone repair in the absence of tumor necrosis factor-alpha signaling [in Eng]. *Cells, Tissues, Organs*. 2001;169(3):285-294.
55. Jaenisch R, Bird A. Epigenetic regulation of gene expression: how the genome integrates intrinsic and environmental signals. *Nat Genet*. 2003;33(Suppl):245-254.
56. Deng P, Yuan Q, Cheng Y, et al. Loss of KDM4B exacerbates bone-fat imbalance and mesenchymal stromal cell exhaustion in skeletal aging. *Cell Stem Cell*. 2021;28(6):1057-1073 e1057.
57. Yi SJ, Jang YJ, Kim HJ, et al. The KDM4B-CCAR1-MED1 axis is a critical regulator of osteoclast differentiation and bone homeostasis. *Bone Res*. 2021;9(1):27.
58. Coffey K, Rogerson L, Ryan-Munden C, et al. The lysine demethylase, KDM4B, is a key molecule in androgen receptor signalling and turnover. *Nucleic Acids Res*. 2013;41(8):4433-4446.
59. Duan L, Chen Z, Lu J, et al. Histone lysine demethylase KDM4B regulates the alternative splicing of the androgen receptor in response to androgen deprivation. *Nucleic Acids Res*. 2019;47(22):11623-11636.
60. Villagra A, Gutierrez J, Paredes R, et al. Reduced CpG methylation is associated with transcriptional activation of the bone-specific rat osteocalcin gene in osteoblasts. *J Cell Biochem*. 2002;85(1):112-122.
61. Huang B, Wang B, Yuk-Wai Lee W, et al. KDM3A and KDM4C regulate mesenchymal stromal cell senescence and bone aging via condensin-mediated heterochromatin reorganization. *iScience*. 2019;21:375-390.